A lightweight hybrid method to estimate the linear acoustic damping of arbitrarily complex geometries

Geoffrey Searby, Aurélie Nicole, Gérard Ordonneau, Mohammed Habiballah

A LIGHTWEIGHT HYBRID METHOD TO ESTIMATE THE LINEAR ACOUSTIC DAMPING OF ARBITRARILY COMPLEX GEOMETRIES

Geoff Searby†, A.Nicole†† G. Ordonneau†† & M. Habiballah††

†*IRPHE, CNRS & Aix-Marseille Université, 13384 Marseilles, France*

†† *ONERA-DEFA, 92322 Châtillon, France*

Abstract

We first recall the classical results for the laminar dissipation of acoustic energy in an acoustic boundary layer. We then show how this result can be used in conjunction with a Helmholtz solver to calculate the laminar damping of a chamber of arbitrary geometry. The approach is validated by application to a trivial geometry for which the result is known analytically. We present results for cases of increasing complexity The computational effort is lightweight, ranging from a few seconds of CPU time for a simple axisymmetric geometry, to a few minutes for a 3-D case with low symmetry. These test cases are non reacting, but the approach can be extended to accommodate strong temperature variations, provided the temperature and density fields are known. Finally we discuss the limitations of this approach.

INTRODUCTION

High frequency instability in liquid-fuelled rocket engines is still an open problem [1,2]. Various methods are used to increase the dissipation rate of acoustic disturbances in rocket engine combustion chambers with the objective of increasing the stability margin of the motors. Among the well-known damping devices are baffles, acoustic liners and quarter-wave resonators. These devices are conceptually simple. Quarter-wave cavities are known to be efficient to increase the stability margin when placed close to the injection plate. However these devices have a relatively narrow dissipation bandwidth and each cavity needs to be tuned to a specific chamber resonance. The optimum tuning of damping cavities and the associated acoustic damping can be calculated analytically only for trivial geometries. For realistic geometries it is necessary to resort to numerical simulation. In this paper we present a simple time-domain method to estimate the total damping rate of an arbitrarily complex geometry.

Two distinct damping mechanisms are associated with acoustic dampers. The first mechanism is diffusive and arises from viscous drag and heat transfer at the cavity walls. This is a linear mechanism, and the associated acoustic resistance is independent of the acoustic amplitude. This mechanism dominates at low acoustic amplitudes and it is important for the *linear* stability of propulsion devices. The second mechanism arises from the formation of vortex eddies at the exit from the damping cavity. This is a nonlinear mechanism and the associated acoustic resistance increases with the velocity of the flow at the entrance to the cavity [3,4,5]. This latter mechanism dominates at high acoustic amplitudes and determines the *dynamic* stability characteristics. The relative contribution of these two mechanisms is described by the acoustic Strouhal number, $\mathrm{St}_{\mathrm{ac}} = \omega R / \hat{u}$, where R is the radius of the cavity exit and $\hat{u}$ is the amplitude of the acoustic velocity at the cavity exit [6]. For $\mathrm{St}_{\mathrm{ac}} >> 1$ the viscous mechanisms dominate. Since the two mechanisms are physically independent, the associated acoustic resistances are additive, at least up to moderately non-linear acoustic levels.

This paper is concerned only with the linear viscous and thermal damping. We first recall the classical results for laminar energy dissipation in an acoustic boundary layer. We then show how this result can be used to calculate the laminar damping of a cavity of arbitrary geometry. This approach is validated on a closed cylindrical cavity, for which the analytical solution is known. We then apply the method to a simple 2–D test case, where we give detailed results. Finally the method is applied to a fully 3–D case. In the conclusion we discuss some possible limitations of the method. The approach described here was originally presented in more detail in a paper published in the Journal of Propulsion and Power [7].

LAMINAR BOUNDARY LAYER THEORY

Viscous and thermal losses at the walls are diffusive and obey qualitatively identical laws. The viscous dissipation is proportional to the product of the velocity gradient at the wall and the shear viscosity. The thermal dissipation is proportional to the product of the temperature gradient at the wall and the thermal conductivity.

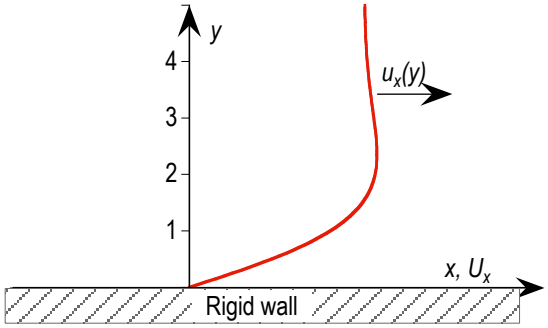

Figure1: Typical velocity profile in an acoustic boundary layer.

Viscous losses

The viscous loss in an acoustic cavity was first calculated by Stokes [8]. Here we will use the boundary layer formulation given by G.K. Batchelor [9].

We consider only the (quasi-)steady state situation, where any time dependence is on a time scale long compared to the acoustic period. We consider a plane infinite wall immersed in a semi-infinite fluid. The y coordinate is normal to the wall, see figure 1. Let the bulk of the fluid oscillate with velocity $u(t) = \hat{u}_x \cos(\omega t)$ parallel to the x axis. If transient effects are neglected, and if the velocity gradients in the direction parallel to the wall are negligible (i.e. if the acoustic wavelength is very large compared to the thickness of the acoustic boundary layer) then it can be shown that the unsteady velocity profile in the liquid is given by

$$u'(y,t) = \hat{u}_x \left[\exp\left(-\frac{y}{\delta_\nu}\right) \cos\left(\omega t - \frac{y}{\delta_\nu}\right) - \cos(\omega t) \right], \tag{1}$$

where δ_ν is a measure of the thickness of the unsteady viscous boundary layer

$$\delta_\nu = \sqrt{\frac{2\nu}{\omega}}, \tag{2}$$

ν is the kinematic viscosity and ω is the angular frequency. The velocity in the fluid oscillates with a highly damped "wavelength" $2\pi\sqrt{2\nu/\omega}$. A typical order of magnitude for the thickness of an acoustic boundary layer is 100µm.

The force per unit area exerted by the wall on the liquid is proportional to the velocity gradient at the wall $F = \rho\nu\left(\partial u'/\partial y\right)\Big|_{y=0}$, and so

$$F = \rho\nu \frac{\hat{u}_x}{\delta_\nu}\left(\sin(\omega t) - \cos(\omega t)\right) \tag{3}$$

It is interesting to note that the force is *not* in phase with the velocity in the bulk of the fluid ($u = \hat{u}_x \cos(\omega t)$): there is a resistive (in phase) component and a reactive (90° phase lag) component. Averaged over an acoustic period, only the resistive component contributes to energy dissipation: $\mathrm{d}E_s/\mathrm{d}t = Fu$.

$$\left\langle \frac{\mathrm{d}E_s}{\mathrm{d}t} \right\rangle_\nu = \frac{1}{2}\rho\nu\frac{\hat{u}_x^2}{\delta_\nu} \equiv \frac{1}{2}\rho\nu\hat{u}_x^2\sqrt{\frac{\omega\nu}{2}}, \tag{4}$$

where E_s is the energy per unit area.

The total rate of energy dissipation by viscous forces in an acoustic cavity can then calculated by integrating equ.(4) over all the solid walls

$$\left\langle \frac{\mathrm{d}E}{\mathrm{d}t} \right\rangle_{\nu} = \int_{\mathrm{s}} \left\langle \frac{\mathrm{d}E_s}{\mathrm{d}t} \right\rangle_{\nu} \mathrm{d}S. \tag{5}$$

Thermal losses

Acoustic oscillations are adiabatic if the wavelength, λ, satisfies $\lambda > 2\pi D_{th}/c \approx 0.5\,\mu m$, where D_{th} is the thermal diffusivity and c is the speed of sound. In combustion chambers this inequality is always true, so the acoustic pressure oscillations give rise to temperature oscillations:

$$\delta T = \frac{\gamma - 1}{\gamma} \frac{T_0}{P_0} \hat{p}, \tag{6}$$

where T_0 and P_0 are the mean temperature and pressure respectively, $\hat{p}$ is the amplitude of the oscillating acoustic pressure, $P = P_0 + \hat{p}\sin(\omega t)$, and γ is the ratio of specific heats. In the presence of an isothermal wall there will be an oscillating heat flux to the wall. This heat flux is irreversible and also contributes to energy dissipation. The calculation for the unsteady heat flux proceeds in a similar way to the calculation of the unsteady viscous stress and was first calculated by Nielsen [10]. The final result for the rate of energy loss per unit area is:

$$\left\langle \frac{\mathrm{d}E_s}{\mathrm{d}t} \right\rangle_{th} = \frac{1}{2} \frac{\gamma - 1}{\gamma} \frac{\hat{p}^2}{P_0} \sqrt{\frac{\omega D_{th}}{2}} \tag{7}$$

where D_{th} is the thermal diffusivity. For a perfect gas, the sound velocity is related to the mean pressure $P_0 = \rho c^2/\gamma$ and in this case equ.(7) is easily written in a form that is symmetrical to equ.(4):

$$\left\langle \frac{\mathrm{d}E_s}{\mathrm{d}t} \right\rangle_{th} = \frac{1}{2}(\gamma - 1) \frac{\hat{p}^2}{\rho c^2} \sqrt{\frac{\omega D_{th}}{2}}. \tag{8}$$

Damping rate

The total rate of acoustic energy dissipation in the system can be calculated by integrating expressions (4) and (8) over the walls acoustic system.

$$\left\langle \frac{\mathrm{d}E_s}{\mathrm{d}t} \right\rangle_{Total} = \int_S \left\langle \frac{\mathrm{d}E_s}{\mathrm{d}t} \right\rangle_{\nu} \mathrm{d}S + \int_S \left\langle \frac{\mathrm{d}E_s}{\mathrm{d}t} \right\rangle_{th} \mathrm{d}S \tag{9}$$

To be rigorous, it is necessary integrate not only over both the walls of the damping cavity, but also over the walls of the combustion chamber. To evaluate these integrals, it is sufficient to know local amplitude of the acoustic velocity and pressure oscillations in front of the wall, but outside the acoustic boundary layer. In the following, we will use the acoustic amplitudes calculated for non-stick (slip) adiabatic walls, and suppose that the velocity distribution outside the boundary layer is not changed by the presence of dissipation. This approximation will be good if the acoustic damping is not too large.

The total acoustic energy in the system can be calculated integrating the kinetic energy, $(1/2)\rho\hat{u}^2$, and the potential energy, $(1/2)\hat{p}^2/(\rho c^2)$, over the volume of the acoustic system:

$$E = \frac{1}{T} \int_T \int_V \left(\frac{1}{2} \rho \hat{u}^2 + \frac{1}{2} \frac{\hat{p}^2}{\rho c^2} \right) \mathrm{d}V \, \mathrm{d}t \tag{10}$$

The integration is over one period of oscillation, $T = 2\pi/\omega$, and over the volume of the system. The damping rate, σ, of *energy* in the system is then given by the ratio of the energy dissipation rate to the total energy:

$$\sigma_E = \frac{1}{E} \frac{\mathrm{d}E}{\mathrm{d}t} \tag{11}$$

Note that the damping rate of the pressure, σ_p, is one-half this quantity

$$\sigma_p = \frac{1}{2}\frac{1}{E}\frac{\mathrm{d}E}{\mathrm{d}t} \tag{12}$$

The damping rate calculated this way is independent of the amplitude of the acoustic wave used to perform the calculations.

APPLICATION TO A CYLINDRICAL RESONATOR

In order to validate the above results, we first apply them to a trivial cylindrical resonator closed at both ends. The cavity is directed along the x axis, and is closed at $x = 0, L$, see figure 2.

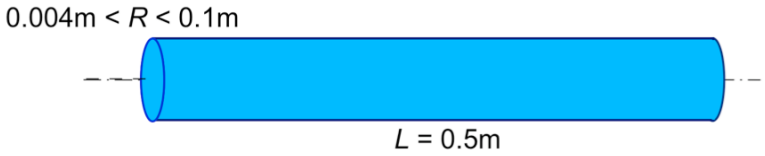

Figure 2: Geometry of the closed cylindrical cavity

If the attenuation is weak then the pressure and velocity in a standing wave can be written

$$\begin{aligned} p(x,t) &= \mathrm{Re}[\hat{p}\cos(kx)\exp(-\mathrm{i}\omega t)] \\ u(x,t) &= -\mathrm{Im}[\mathrm{i}\hat{u}\sin(kx)\exp(-\mathrm{i}\omega t)] \\ \hat{p} &= \rho c\hat{u} \end{aligned} \tag{13}$$

where $\hat{p}$ and $\hat{u}$ are the peak amplitudes of the oscillations at the anti-nodes of velocity and pressure respectively. If the attenuation is weak, they may be considered constant during a period of oscillation. The integral in equ.(10) for the total energy in the cylinder is then easily evaluated to give:

$$E = \frac{1}{4}\pi R^2 L\rho\hat{u}^2 \equiv \frac{1}{4}\pi R^2 L\frac{\hat{p}^2}{\rho c^2} \tag{14}$$

Viscous contribution

The viscous contribution to damping is given by the integral of equ.(4) over the side walls of the cylinder. There is no contribution from the end walls, since the velocity there is zero.

$$\left\langle \frac{\mathrm{d}E}{\mathrm{d}t} \right\rangle_{\nu} = \frac{1}{2}\pi RL\rho\hat{u}^2\sqrt{\frac{\omega\nu}{2}} \tag{15}$$

The viscous contribution to the damping rate, $\sigma_\nu = (1/E)(\mathrm{d}E/\mathrm{d}t)_\nu$ is then

$$\sigma_\nu = \frac{2}{R}\sqrt{\frac{\omega\nu}{2}} \tag{16}$$

Thermal contribution

The thermal contribution to damping is given by the integral of equ.(8) over the side walls of the cylinder. The integral must also be evaluated at the end wall(s), if the cylinder is closed, since these locations are anti-nodes for the oscillations of pressure and temperature.

$$\left\langle \frac{\mathrm{d}E}{\mathrm{d}t} \right\rangle_{th} = \pi RL(\gamma-1)\frac{1}{2}\frac{\hat{p}^2}{\rho c^2}\sqrt{\frac{\omega D_{th}}{2}}\left(1+\frac{2R}{L}\right) \tag{17}$$

The thermal contribution to the damping rate is then:

$$\sigma_{th} = \frac{2(\gamma-1)}{R}\sqrt{\frac{\omega D_{th}}{2}}\left(1+\frac{2R}{L}\right) \tag{18}$$

Total damping of a cylindrical resonator

The total damping rate of energy is just the sum of the viscous and thermal contributions, $\sigma_e = \sigma_\nu + \sigma_{th}$:

$$\sigma_e = \frac{2}{R}\left[\sqrt{\frac{\omega\nu}{2}} + (\gamma-1)\sqrt{\frac{\omega D_{th}}{2}}\left(1+\frac{2R}{L}\right)\right] \quad (19)$$

Equation (19) gives the damping rate of *energy* in the cavity. The damping rate of *pressure* is one half the damping rate of energy :

$$\sigma_p = \frac{1}{R}\sqrt{\frac{\omega\nu}{2}}\left[1+\frac{(\gamma-1)}{\sqrt{\mathrm{Pr}}}\left(1+\frac{2R}{L}\right)\right] \quad (20)$$

where we have expressed the thermal diffusivity in terms of the viscosity and the Prandtl number. This expression is valid for weak damping. Equivalent expressions have been obtained by other authors, such as Tijdeman [11], using a more rigorous formulation.

In order to validate this approach, we calculate the damping rate of the cylinder analytically for varying values of the radius and compare the results with the damping rate obtained from direct numerical simulation in the time domain with resolved boundary layers. For the validation calculation, we have used gas properties that are representative of a rich hydrogen-oxygen flame at 1Mpa with a mixture ratio of 2.1. The physical properties of the gas are shown in table 1. The undamped eigenfrequency of the cylinder is just $f_0 = c/2L = 1884.5\,\mathrm{Hz}$

To first-order, the frequency of the damped cavity, f, can be obtained from the undamped eigenfrequency f_0 using the relation $f = f_0 - \sigma_p/(2\pi)$:

T (K)	2100	*c* (m/s)	1884.5
ρ (kg/m3)	0.358	γ	1.27
μ (kg/m/s)	$4.833\ 10^{-5}$	*v* (m^2 /s)	$1.35\ 10^{-4}$
Cp (J/kg/K)	6257.6	Pr	0.79

Table 1: Properties of gas used to calculate the damping of a closed cylinder

Figure 3 shows the calculated pressure damping rates of the fundamental mode of the closed cylinder with both isothermal and adiabatic (no heat transfer) walls for a range of cavity radii. The green cross is the result of a DNS temporal simulation performed with the ONERA CEDRE code. In this simulation the viscous boundary layers were fully resolved with a mesh size of 7.55μm in the radial direction, however the walls were considered to be isothermal. For the point considered, the damping rate found by DNS simulation, 178.5 s^{-1}, is in excellent agreement with the analytical evaluation presented above, 178.8 s^{-1}, and validates the approach.

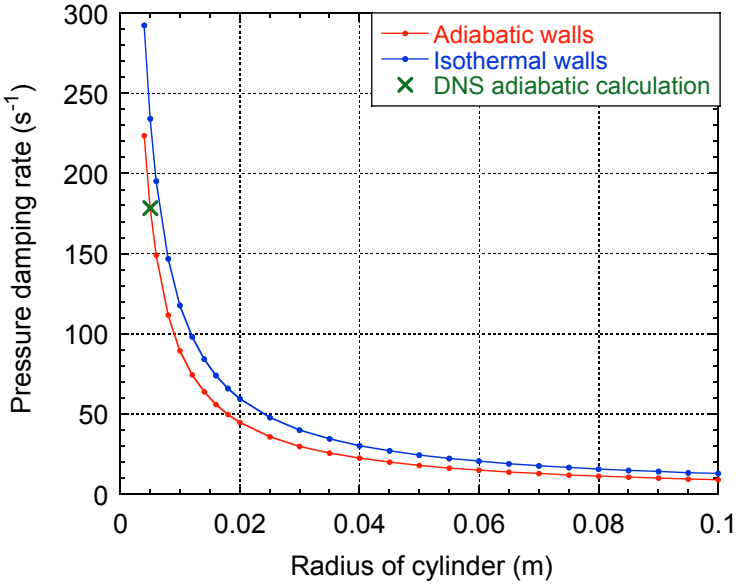

Figure 3 Damping rate of a closed cylinder with adiabatic and isothermal walls. The green cross is an adiabatic DNS simulation performed using the ONERA CEDRE code with fully resolved viscous boundary layers

APPLICATION TO NON TRIVIAL GEOMETRIES

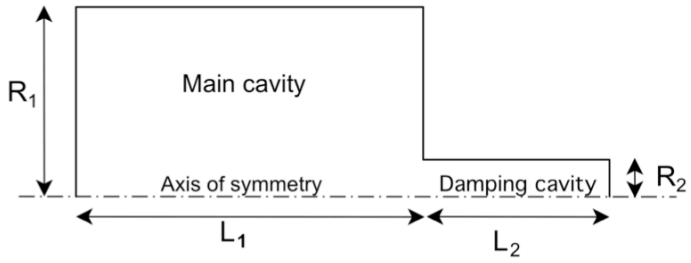

Figure 4: Simple geometry of two coupled cylindrical cavities

Analytical expressions, such as (13), for the spatial distribution of the acoustic field can be found only for trivial geometries and are not available for more realistic geometries. To the best of our knowledge even the simple axisymmetric geometry shown in figure 4 does not have a known analytical solution. However it is possible to obtain a numerical solution using a standard software tool to solve the Helmholtz equation.

The Helmholtz equation

The standard wave equation (d'Alembert's equation) for small amplitude acoustic propagation in a lossless medium is

$$\frac{\partial^2 p}{\partial t^2} - c^2 \nabla^2 p = 0, \tag{21}$$

where p is the unsteady acoustic pressure and c is the speed of sound in the medium. If the acoustic oscillation is harmonic and quasi-stationary, such as at resonance, the spatial and time dependencies of the acoustic field can be separated:

$$p(\mathbf{x},t) = \hat{p}(\mathbf{x})\exp(-\mathrm{i}\omega t) \tag{22}.$$

The space-dependent part of the acoustic pressure field, $\hat{p}(\mathbf{x})$, must then satisfy Helmholtz's equation:

$$\nabla^2 \hat{p}(\mathbf{x}) + \frac{\omega^2}{c^2}\hat{p}(\mathbf{x}) = 0, \tag{23}$$

where ω is now an eigenvalue of the problem. This differential equation is easily solved using standard software tools. The necessary inputs are

- The speed of sound (which can be a function of position)
- The boundary conditions

The outputs are

- The eigenfrequencies, ω_n of the geometry defined by the boundary conditions
- The pressure field $\hat{p}(\mathbf{x})$ and the velocity field $\hat{u}(\mathbf{x})$ where

$$\hat{u}(\mathbf{x}) \equiv \frac{\mathrm{i}}{\omega_n \rho}\hat{p}(\mathbf{x}).$$

The numerical solutions for the pressure and velocity fields can then be used as before to calculate the total energy in the system:

$$E = \frac{1}{2}\int_V \left(\frac{1}{2}\rho\hat{u}^2(\mathbf{x}) + \frac{1}{2}\frac{\hat{p}^2(\mathbf{x})}{\rho c^2}\right)\mathrm{d}x\,\mathrm{d}y\,\mathrm{d}z \tag{24}$$

and the total energy dissipation at the walls:

$$\left\langle \frac{\mathrm{d}E}{\mathrm{d}t} \right\rangle = \frac{1}{2}\sqrt{\frac{\omega_n \nu}{2}}\int_S \left(\rho\hat{u}_s^2(\mathbf{x}) + \frac{(\gamma-1)}{\sqrt{\mathrm{Pr}}}\frac{\hat{p}_s^2(\mathbf{x})}{\rho c^2}\right)\mathrm{d}s \tag{25}$$

where $\hat{u}_s$ and $\hat{p}_s$ are the values of the velocity and pressure at the walls. The pressure damping rate is then given by equation (12). The solutions to the Helmholtz equation can be obtained in a few seconds for a simple 2–D geometry, or in a few minutes for a 3–D geometry.

The association of a Helmholtz solver to obtain the lossless acoustic modes of an arbitrary chamber, and analytical boundary layer theory to calculate the associated acoustic damping will be called the "hybrid model".

In the following sections of this paper, the Helmholtz equation has been solved using a commercial PDE solver called COMSOL. As a first step we apply it to the geometry of figure 4. This is an axisymmetric geometry in which a large cylinder is acoustically damped by a smaller cylinder. The dimensions of the main chamber are: L_1 = 0.2m, R_1 = 0.11m. The dimensions of the small cylinder will be varied around the classical "$\lambda/4$" tuning. The physical properties of the gas in the system are the same as in the previous section (table 1) except for the kinematic viscosity which has been increased by a factor 25, from 1.35 10^{-4} to 3.375 10^{-3} m^2/s in order to limit the CPU time required for the DNS calculations that are used for comparison.

The hybrid model for this geometry has an unstructured triangular mesh, with typically 6 000 to 7 000 cells, depending on the size of the damping cavity. Figure 5 shows typical solutions for the pressure fields of the first and second acoustic modes of figure 4. The flow streamlines are shown in red and the relative contributions for the damping from each wall are also indicated. Since the walls are adiabatic in this test, there is no thermal dissipation and the two extremities do not contribute to the damping. It is interesting to note that, the damping on the main cavity walls represents 9% of the damping for mode 1, and 34% of the total damping for mode 2.

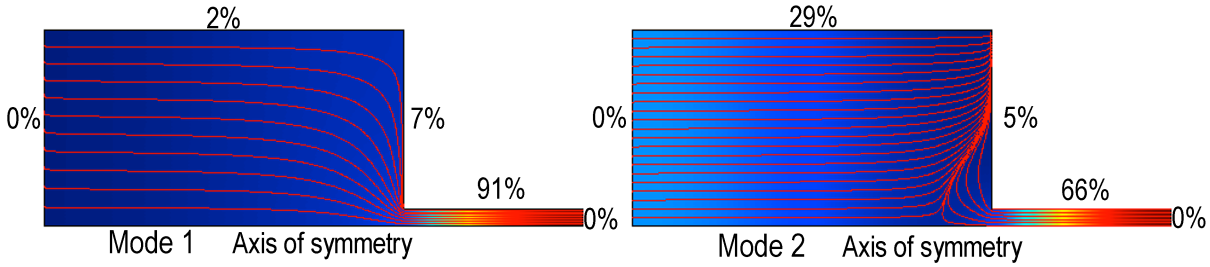

Figure 5: Typical acoustic pressure fields for the geometry of figure 3. L_1 = 0.2 m L_2 = 0.1 m R_1 = 0.11 m R_2= 0.019 m.

Figure 6 shows the evolution of the frequencies and damping of the first two modes as a function of the damping cavity radius. The length of the damping cavity is 0.1 m, corresponding to the "standard" λ/4 tuning with respect to the first mode of the main cavity. Mode 1 is more strongly damped than mode 2. A closer investigation shows that the reason for this difference is that the relative acoustic amplitude in the damping cavity is systematically higher for mode 1 than for mode 2, leading to a higher dissipation in the damping cavity. The results also predict that the total damping rate increases as the radius of the damping cavity is decreased.

The physical reason for this is that the resulting increase in relative acoustic intensity inside the damping cavity more than overweighs the decrease in surface area. Obviously, this trend cannot continue indefinitely and the semi-analytical hybrid analysis will fail at small cavity radii when boundary layer thickness becomes comparable to cavity radius.

Figure 7 shows the undamped eigenfrequencies and the damping rates of the first two modes as a function of the length of the damping cavity, for a damping cavity radius R_2 = 0.01 m. The resonant frequencies of the coupled system are, in general, different to those of the isolated components. The resonant frequencies evolve in a very non-linear manner with a change in the length of the damping cavity. This behaviour is generic, and is consistent with a simple quasi 1–D analytical model of two coupled cavities [12]. It will be seen that the resonant frequencies of a more complex 3-D geometry also evolves in a similar manner with the length of the damping cavity. The evolution of the damping rates of the first two modes is shown in the fig.6b. The λ/4 tuning is not optimal for the damping of mode 1. In fact

it is a dangerous tuning since the damping rate varies very quickly with cavity length (or with a change in sound speed in one of the cavities). A better tuning for damping mode 1 would be λ/3.5 (L_2 = 0.115 m) instead of λ/4. Another interesting tuning is λ/1.3 (L_2= 0.320 m). For this cavity length, mode 1 is almost as strongly damped as with the λ/4 tuning, but mode 2 is also strongly damped and moreover the damping rates of both modes are relatively insensitive to cavity length.

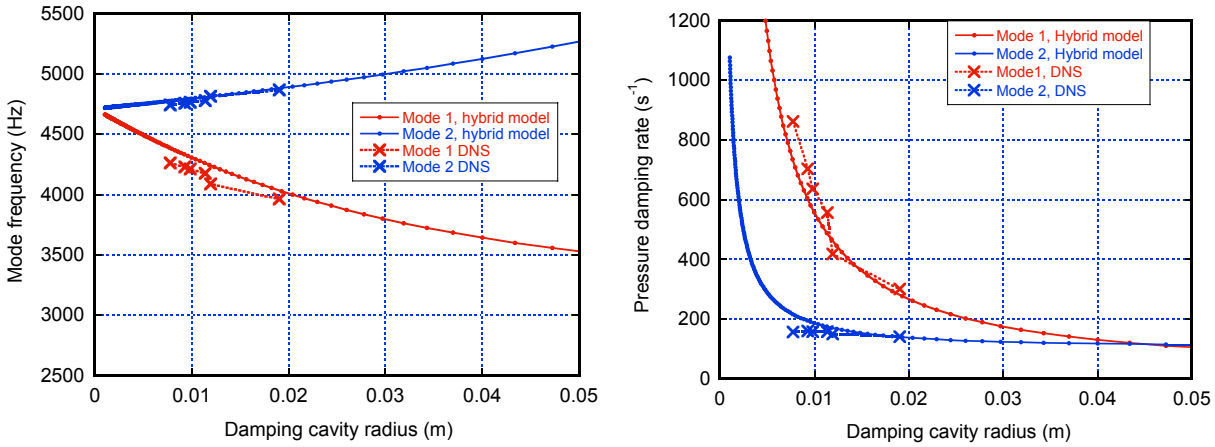

Figure 6: Evolution of mode frequencies and damping rate as functions of damping cavity radius. L_1 = 0.2m L_2 = 0.1m R_1 = 0.11m R_2 variable. Kinematic viscosity = 3.375 10^{-3} m^2/s. The small markers are the hybrid model, The crosses are from DNS using the ONERA CEDRE code.

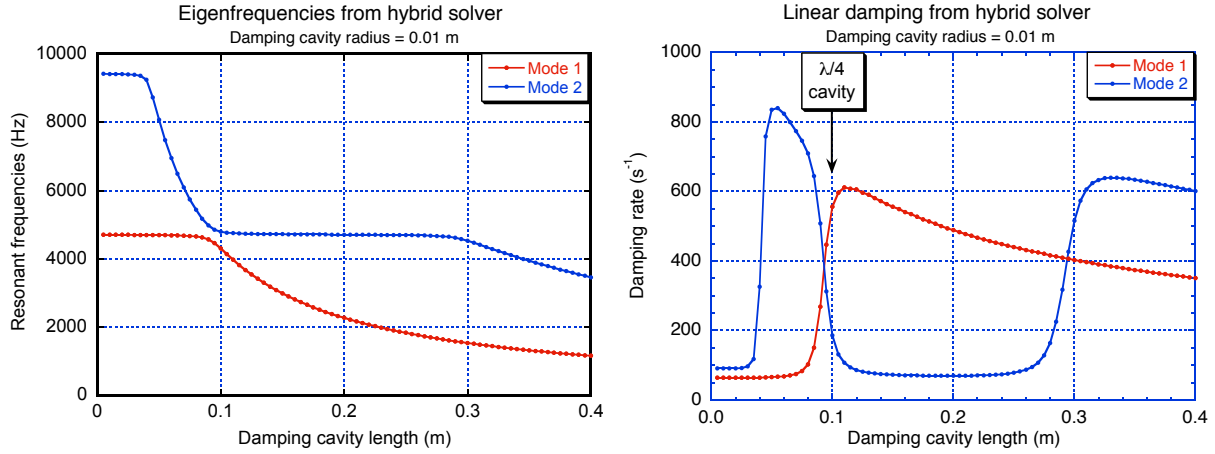

Figure 7: Evolution of mode frequencies and damping rates as functions of damping cavity length. L_1 = 0.2 m L_2 variable R_1 = 0.11 m R_2 = 0.01 m. Kinematic viscosity = 3.375 10^{-3} m^2/s.

APPLICATION TO A 3–D LABORATORY COMBUSTION CHAMBER

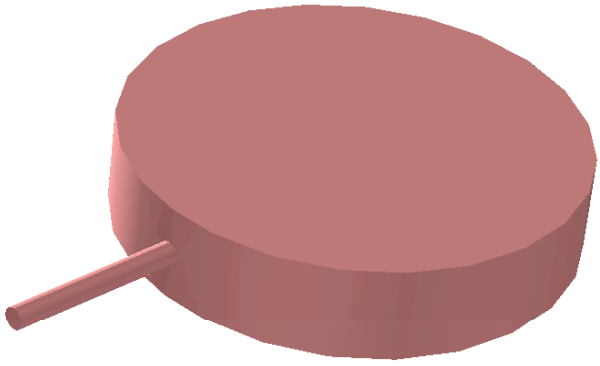

Figure 8: Geometry of the combustion chamber.

We have applied the hybrid model to the 3-D Common Research Chamber (or CRC) used in the frame of the REST French-German research initiative into high frequency combustion instability [13]. The CRC is a small aspect ratio cylindrical chamber equipped with a coaxial injector, an igniter, quartz windows, pressure sensors and a lateral damping cavity. The chamber radius is 100mm and the chamber length is 42mm. It is equipped with a cylindrical damping cavity of radius 5mm and variable length between 0mm and 160mm. The geometry is shown in figure 8. The CRC and damping cavity has been modelled in 3–D, but excluding the injector and the igniter. Since the objective here is to simulate the damping of a real combustion chamber, all the walls are isothermal. The mesh is unstructured with typically 70 000 to 80 00 cells, depending on the length of the damping cavity. The execution time of the Helmholtz solver was approximately 5 minutes per geometry, including post-processing to obtain the damping rates. The properties of the gas used in these calculations are those of ambient air at 20°C:

γ	1.41	c (m/s)	345
ρ (kg/m3)	1.2	Pr	0.773
μ (kg/m/s)	$2.04\ 10^{-5}$	ν (m^2 /s)	$1.70\ 10^{-5}$

Table 2 Properties of ambient air used to calculate the mode frequencies and damping of the CRC

Figure 9a shows the first six eigenfrequencies of the 3–D chamber as a function of the cavity length. The behaviour is qualitatively identical to that of the axisymmetric coupled chambers, figure 7. However, the presence of the damping cavity breaks the orientationally degenerate transverse modes into two distinct modes labelled "σ" and "π" modes, see figure 10.

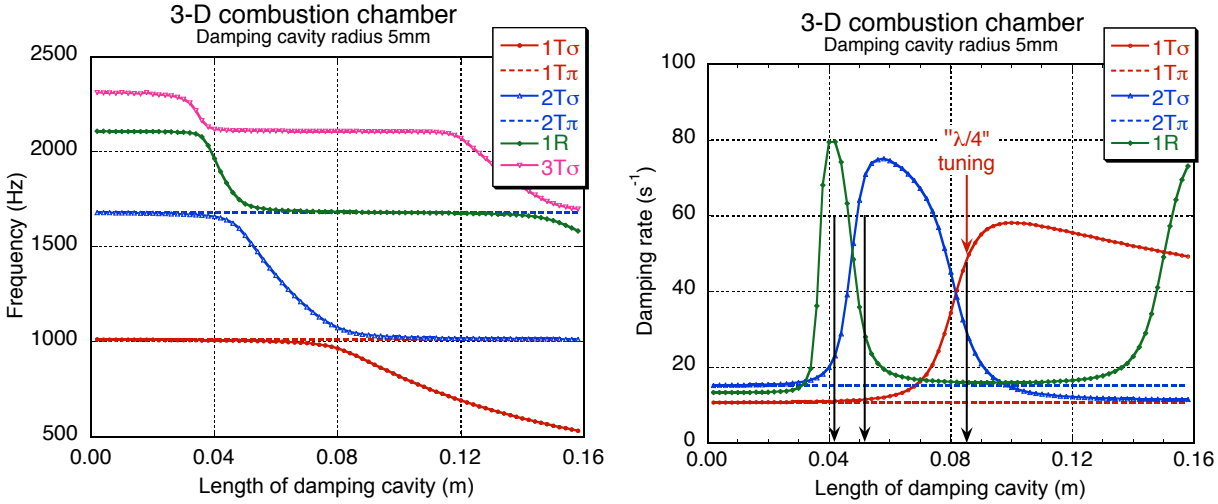

Figure9: Mode frequencies and damping rates of the first 6 modes of the 3–D CRC as a function of the cavity length, for ambient air and isothermal walls.

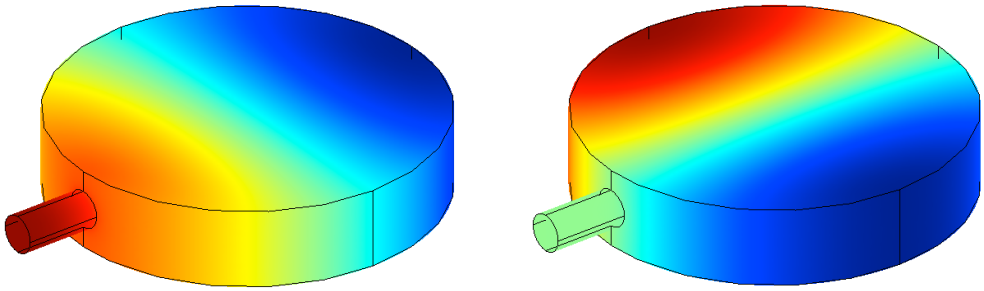

Figure 10. 1Tσ and 1Tπ modes of the REST chamber equipped with a single damping cavity.

The "π" modes have a pressure node aligned with the axis of the damping cavity. There is no flow into or out of the cavity, and the frequency of the mode is not affected by the presence of the cavity. The "σ" modes are orthogonal to the "π" modes. They have a pressure anti-node aligned with the axis of the damping cavity, and they are strongly affected by its length. The modes with a radial parent do not have a "π" form and also change in frequency with the length of the cavity.. The frequencies of the "σ" modes do not change linearly with cavity length, but tend to change rapidly for certain critical lengths of the

cavity. The modes have been labelled according to the shape of the "parent" mode, i.e. the shape of the mode, as the length of the cavity tends to zero.

Figure 9b shows the damping rate of the first five modes as a function of the cavity length. Again the behaviour is qualitatively identical to that of the axisymmetric coupled chambers, figure 7. The black arrows show the lengths of cavities tuned to the standard "$\lambda/4$" length for the 1T, 2T and 1R chamber modes. The cavity length L_R=41mm is well adapted to damp the 1R mode. However it is clear that the cavity lengths L_R =51mm and 85mm are not optimal to damp the 2Tσ and 1Tσ modes. Contrary to the 2–D case, there is no single cavity length that provides good damping of both the 2Tσ and 1Tσ modes. The damping of the nTπ modes is insensitive to the length of the damping cavity.

The experimental values for measured damping rate of the REST combustion chamber are reported and discussed in the paper presented by M. Oschwald et al. [14]

DISCUSSION

Are these results reliable?

There is no problem with numerical accuracy: the numerical results agree very closely (≪ 1‰) with the analytical solution, when the latter is known (2-D rectangle, 2-D disk, axisymmetric cylinder...). It has been verified that the numerical results are independent of the mesh resolution for the meshes used here. It thus is expected that there is no significant numerical error for the non-trivial geometries

Possible sources of error thus lie in the analytical expressions that have been used to compute the damping rates. The analysis has two components:

- Boundary layer theory
- Eigenmode acoustic analysis

The corresponding analytical expressions are exact, but with a number of restrictions such as:

- No mean flow
- Small amplitude acoustics
- Small damping rate compared to the frequency

We will first examine the hypotheses and approximations used in the boundary layer theory.

Approximations and limitations arising from boundary layer theory

1) Boundary layer theory used here supposes that the acoustic pressure and velocity are invariant by translation along the walls. The equivalent approximation is that the acoustic wavelength is very large compared to the boundary layer thickness. This (quasi 1-D) approximation is good for real systems.

2) Boundary layer theory supposes that the acoustic medium is semi-infinite. The equivalent approximation is that the boundary layer thickness negligible compared to all cavity dimensions. This approximation is good for real systems

3) Effect of turbulence is neglected. The turbulence level inside damping cavities is low, so this will not be a problem. Elsewhere it is probably not important provided that the Kolmogoroff scale is considerably greater than the acoustic boundary layer thickness.

4) Temperature and composition gradients are neglected. The mean-flow boundary layers are much thicker than the acoustic boundary layers, so one should use the gas properties calculated at the wall temperature (supposed known) and not the mean burnt gas properties in the bulk of the chamber.

5) The effect of mean flow is neglected. There is no mean flow in damping cavities, so it is not a problem there. However but it will change the calculated contribution of damping by combustion chamber walls.

6) The effect of cross flow at cavity exit is neglected.

Approximations and limitations arising from eigenmode analysis

1) The frequencies given by the Helmholtz solver are (undamped) eigenfrequencies. The real frequencies of damped systems have smaller values. The first order correction for the frequency shift of

an acoustic resonator, due to damping, is $f = f_0 - \sigma_p/(2\pi)$, where f_0 is the undamped eigenfrequency. This correction can easily be included.

2) The flow fields are calculated neglecting the flow resistance (due to dissipation) at cavity entrance. The amplitude of the acoustic wave inside the cavity will be over-evaluated when cavity entry resistance is higher than the entry reactance. As a consequence, the damping produced by the cavity walls will also be over-estimated. The expected ratio of over-evaluation is $(R^2 + \chi^2)/\chi^2$ where R and χ are the cavity resistance and reactance. The equivalent cavity entrance resistance can be computed from the dissipation rate and the local acoustic velocity at the cavity entrance [7]. These are known quantities.

3) The Helmholtz equation is exact in the limit of vanishingly small acoustic amplitude. The acoustic flow is then the solution of a potential equation and is thus irrotational. Boundary layer separation and recirculation zones in the acoustic flow are thus totally excluded. For a finite acoustic amplitude, boundary layer separation will occur at sharp edges, such as the exit of a damping cavity. At low acoustic amplitude, the power is dissipated by recirculation at the cavity exit is negligible in comparison with the dissipation at the chamber walls.

However comparison with numerical simulation shows that boundary layer separation at the cavity exit also modifies the shape of the acoustic flow field, and hence the modifies the distribution of velocity and pressure along the walls. Boundary layer separation thus modifies the damping rate by changing the velocity and pressure distribution along the walls. This phenomenon is probably the greatest source of error identified so far.

The above remarks concerning the comparison between this approach and DNS will also apply to the comparison with experimental measurements on the CRC.

5) In real experiments non-linear damping (acoustic jets) will occur if the acoustic displacement at the cavity exit is of the order, or greater than the cavity radius [15]. This linear limit can also be written $u/\omega < R_{\text{cavity}}$

6) There is no mean flow. It is well known that resonant frequencies are modified by mean flow in the chamber. Acoustic flow, wall gradients and damping will also be modified It would be possible to account for some Mach effects by solving the aero-acoustic equations instead of the Helmholtz equation. This has not been done yet.

7) The analysis has supposed that there is no turbulence and no inhomogeneities. Large-scale temperature and density variations can be included in the Helmholtz solver (although it has not been necessary here).

8) The effect of an exhaust nozzle was not taken into account. At present it is not possible to model a choked exhaust nozzle. However it is possible to specify a wall impedance (if known) in replacement of the nozzle.

CONCLUSIONS AND PERSPECTIVES

A combination of laminar boundary layer theory and a solver for the Helmholtz equation has been used to provide a simple lightweight method to estimate linear damping rate of a combustion chamber with a damping cavity. The method is applicable to arbitrary complex geometries. The necessary CPU time is of the order of a few seconds for a simple 2-D geometry and of the order of a few minutes for a simple 3–D chamber with one damping cavity. It would not be difficult to apply the method to a combustion chamber equipped with a damping ring of n cavities.

This approach has been validated by DNS for the trivial geometry of a regular cylinder closed at both ends. The approach is strictly laminar, but the thin acoustic boundary layer should remain laminar even for turbulent flows. However the method does not take account effect of boundary layer separation and recirculation on mode shape and velocity distributions. It does not include the contribution of other non-linear phenomena, such as the formation of acoustic jets at high acoustic amplitudes.

The approach can easily be extended to include space dependant gas properties (temperature, composition). It is also possible to imagine that that this frequency domain approach could be coupled to

a time domain code. The frequency domain code could provide damping information to the time domain code (to be modelled by some impedance condition, for example), and the time domain code could provide density and temperature fields for the frequency domain code.

REFERENCES

[1] D.T. Harrje and F.H. Reardon. *Liquid propellant rocket combustion instability*. Technical Report **SP-194**, NASA, Washington, DC, 1972.

[2] V. Yang and W. Anderson. *Liquid rocket engine combustion instability*, volume **169** of Progress in Astronautics and Aeronautics. AIAA, Washington DC, 1995.

[3] Uno Ingard and Hartmut Ising. *Acoustic nonlinearity of an orifice*. Journal of the Acoustical Society of America, **42**(1):6–17, 1967.

[4] P. K. Tang and W. A. Sirignano. *Theory of a generalized helmholtz resonator*. Journal of Sound and Vibration, **26**(2):247–262, 1973.

[5] P. K. Tang, D. T. Harrje, and W. A. Sirignano. *Experimental verification of the energy dissipation mechanism in acoustic dampers*. Journal of Sound and Vibration, **26**(2):263–267, 1973.

[6] M.C.A.M. Peters, A. Hirschberg, A.J. Reijnen, and A.P.J. Wijnands. *Damping and reflection coefficient measurements for an open pipe at low Mach and low Helmholtz numbers*. Journal of Fluid Mechanics, **256**:499–534, 1993.

[7] Geoffrey Searby, Aurélie Nicole, Mohammed Habiballah, and Emmanuel Laroche. *Prediction of the efficiency of acoustic damping cavities*. Journal of Propulsion and Power, **24**(3): 516–523, 2008.

[8] G. G. Stokes. *On the communication of vibration from a vibrating body to a surrounding gas*. London, Edinburgh and Dublin Philosophical Magazine and Journal of Science, 4th series, **36**(245):401–421, 1868.

[9] G.K. Batchelor. *An introduction to fluid dynamics*. Cambridge University Press, 1967.

[10] A. K. Nielsen. *Acoustic resonators of circular cross-section and with axial symmetry*. Transactions of Danish Academy of Technical Sciences, **10**:9–70, 1949.

[11] H. Tijdeman. *On the propagation of sound in cylindrical tubes*. Journal of Sound and Vibration, **39**:1–33, 1975.

[12] M.Oschwald, Z. Faragó, G. Searby, and F. Cheuret. *Resonance frequencies and damping of a cylindrical combustor acoustically coupled to an absorber*. Journal of Propulsion and Power, **24**(3):524–533, 2008.

[13] REST: ***R***ocket ***E***ngine ***S***tability research ini***T***iative. http://rest.cnes.fr/

[14] M. Oschwald, M. Marpert, *On the acoustics of rocket combustors equipped with quarter wave absorbers*. EUCASS09, 6-9 July Versailles,France , 2009

[15] I. V. Lebedeva and A. E. Grushin. *Amplitude and frequency characteristics of acoustic jets*. Acoustical Physics, **46**(3):359–364, 2003.